Supporting information for:

Theoretical Design and Experimental Implementation of Ag/Au Electrodes for the Electrochemical Reduction of Nitrate

Federico Calle-Vallejo[a, †], Minghua Huang[b, †], John B. Henry[b], Marc T. M. Koper[a,*], Aliaksandr S. Bandarenka[b,*]

[a] Leiden Institute of Chemistry, Leiden University, PO box 9502, 2300 RA Leiden, The Netherlands
[b] Center for Electrochemical Sciences, Ruhr-Universität Bochum, Universitätstr. 150, D-44780, Bochum, Germany

† F. Calle-Vallejo and M. H. Huang contributed equally to this article.

* m.koper@lic.leidenuniv.nl (M. Koper); *aliaksandr.bandarenka@rub.de (A.S. Bandarenka)

Table of Contents:

1. DFT Calculations

1.1. Gas-phase Correction: The DFT binding energies of nitrate are initially calculated with respect to hydrogen and nitric acid in gas phase, as shown in Equations (S1) and (S2):

$$* + HNO_3 \rightarrow *NO_3 + \frac{1}{2} H_2 \quad \text{(S1)}$$

$$\Delta E_{NO_3}^{DFT} = E_{*NO_3} + \frac{1}{2} E_{H_2} - E_* - E_{HNO_3} \quad \text{(S2)}$$

Here * denotes an active site in the surface and $*NO_3$ represents the adsorbed nitrate group. The choice of a gas reference based on HNO_3 and H_2 instead of using dissolved NO_3^- is due to the difficulties to describe accurately the electronic states, solvation effects and thus the energies of the latter within DFT.

In Table S1, we present the gas-phase and adsorbed-state data needed to compute the free energies of adsorption at standard conditions of pressure and temperature, taking into account that $\Delta G = \Delta E_{DFT} + \Delta ZPE - T\Delta S$. In the particular case of $*NO_3$, only vibrational entropy effects were taken into account as they are normally the largest contribution for adsorbed species to the total entropy (some authors even neglect all kinds of entropy contributions for adsorbed species, see Ref. [1]).

Table S1. Data for gas-phase H_2 and HNO_3 and adsorbed $*NO_3$. The experimental data are marked in bold and taken from Ref. [2]. The rest of the data were obtained with DFT through vibrational analyses.

Species	ZPE / eV	TS / eV
H_2 (g)	0.27	**0.40**
HNO_3 (g)	0.69	**0.82**
$*NO_3$ (ads)	0.38	0.31

Moreover, it is worth noting that PBE has a marked limitation in its description of the energetics of molecules containing multiple bonds between atoms [3], such as those having O-N-O backbones. In Table S2, we present a list of selected N-, H-, and O-containing molecules, from which it is evident there exists a large overbinding in all O-N-O containing molecules that causes important differences between experimental and DFT-calculated formation energies. It is noteworthy that the error increases as more oxygen atoms are present in the molecules and that the predictions improve as hydrogen is added to them, i.e. as multiple bonds are reduced to simple bonds. Particularly, the error for in the formation energy

of HNO_3 is around 1.12 eV, and thus we corrected our DFT-calculated free energies by that number. **It should be noted that though this correction strengthens the actual values of the adsorption energies, it has no influence over the trends as it is only a constant shift applied to all values. Furthermore, the fact that standard DFT does not describe well HNO_3 in gas phase does not imply that the binding energies of $*NO_3$ presented here are wrong.**

Table S2. Comparison between experimental and DFT-predicted free energies of formation. The experimental data (TS) are marked in bold and taken from Ref. [4], the zero-point energies (ZPE) were calculated with DFT through vibrational analyses.

species	ZPE / eV	TS / eV	ΔG^0_{DFT} / eV	ΔG^0_{EXP} / eV	$\left\|\Delta G^0_{EXP} - \Delta G^0_{DFT}\right\|$ / eV
NH_3 (g)	0.91	**0.60**	-0.35	-0.17	0.18
N_2H_4 (g)	1.39	**0.74**	1.33	1.65	0.32
NO (g)	0.12	**0.65**	0.72	0.90	0.18
NO_2 (g)	0.24	**0.74**	-0.43	0.53	0.96
N_2O_4 (g)	0.61	**0.94**	-1.11	1.01	2.12
HNO_2 trans (g)	0.53	**0.77**	-1.16	-0.46	0.71
HNO_2 cis (g)	0.53	**0.77**	-1.14	-0.43	0.71
HNO_3 (g)	0.69	**0.82**	-1.88	-0.77	1.12

The relationship between DFT energies and free energies in the gas-phase scale, including the correction of 1.12 eV, is given in Equation S3.

$$\Delta G^{DFT}_{NO_3} = \Delta E^{DFT}_{NO_3} - 0.979 \qquad \text{(S3)}$$

1.2. Electrochemical Scale for the Adsorption Energies: we converted our DFT-calculated adsorption energies by means of Hess' Law and the free energy diagram shown in Figure S1. The number 0.075 eV in that figure is obtained taking into account that the standard formation energies of HNO_3 in liquid and gas phases are -0.836 eV and -0.762 eV, respectively. Furthermore, the number 0.317 eV is obtained by the combination of -0.836 eV, i.e. the formation energy of liquid nitric acid, and the standard formation energy of the NO_3^- species in aqueous solutions, which is -1.153 eV. These values were taken from Ref. [2].

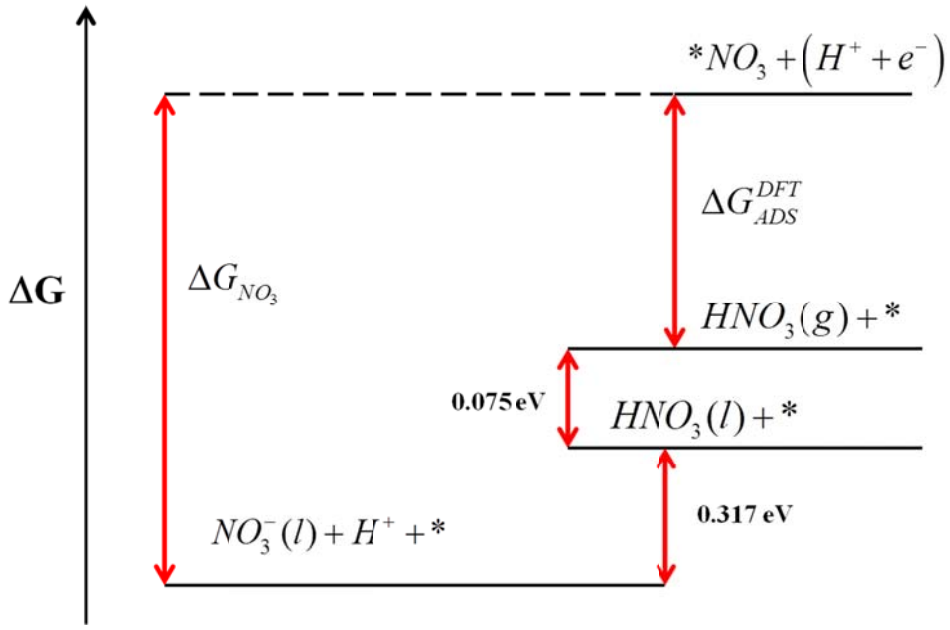

Figure S1. Free energy diagram relating the energetics of HNO_3 in liquid and gas phases and dissolved and adsorbed NO_3^-, at pH = 0. The experimental data (0.075 eV and 0.317 eV) were taken from Ref [2].

The experimental data were taken from Ref. [2]. From this diagram, it is possible to conclude that the adsorption energies of Equation S4, i.e the adsorption energies on the electrochemical scale ($\Delta G_{NO_3}^{EC}$), are related to those calculated with DFT ($\Delta G_{NO_3}^{DFT}$) through Equation (S5).

$$* + NO_3^-(l) \rightarrow *NO_3 + e^- \quad \text{(S4)}$$

$$\Delta G_{NO_3}^{EC} = \Delta G_{NO_3}^{DFT} + 0.392 \quad \text{(S5)}$$

The combination of Equations S3 and S5 provides the relationship between DFT binding energies and free energies of adsorption in the electrochemical scale, Equation S6.

$$\Delta G_{NO_3}^{EC} = \Delta E_{NO_3}^{DFT} - 0.587 \quad \text{(S6)}$$

1.3. Adsorption Energies and Active Sites: Table S3 contains the binding energies and the free energies of adsorption from Eqns S2 and S6 on Au and Ag and Ag/Au NSAs and SAs. The numbers in yellow (Au), blue (Ag) and green (Ag/Au) were used in Fig. 3 in the article. Table S3 also contains coordination numbers (CN) the type of cells and the k-point samplings (kps) used.

Table S3. Binding energies and free energies of adsorption of NO_3 on various surfaces. a) 111 Surfaces: 2×2 unit cells for the NSAs and SAs (kps: 6×6×1) and 3×3 unit cells for the surfaces with adatoms (kps: 4×4×1). CN: 9 for the terraces and 4 for the adatoms (3 bonds with the surface plus one with the other adatom).

system	$\Delta E_{NO_3}^{DFT}$	$\Delta G_{NO_3}^{EC}$
Pure Au	1.00	0.42
NSA 25% Ag	1.02	0.43
NSA 50% Ag	0.98	0.40
NSA 75% Ag	0.97	0.38
NSA 100% Ag	0.99	0.40
SA 25% Ag	0.83	0.24
SA 33% Ag	0.64	0.05
SA 50% Ag	0.62	0.03
SA 75% Ag	0.53	-0.06
SA 100% Ag	0.26	-0.32
Pure Ag	0.32	-0.27
1Ag adatom in Au(111)	0.42	-0.17
2Ag adatoms in Au(111)	-0.35	-0.93
2 Au adatoms in Au(111)	0.06	-0.53
2 Ag adatoms in Ag(111)	-0.28	-0.87

b) 2-atom wide 211 surfaces (kps: 6×6×1). CN: 7 at the step edge.

System	$\Delta E_{NO_3}^{DFT}$	$\Delta G_{NO_3}^{EC}$
Pure Au	0.55	-0.04
NSA 33% Ag	0.63	0.04
NSA 50% Ag	0.56	-0.03
NSA 66% Ag	0.55	-0.03
NSA 100% Ag	0.61	0.03
SA 33% Ag	0.22	-0.37
SA 50% Ag	0.14	-0.45
SA 66% Ag	0.12	-0.47
SA 100% Ag	0.00	-0.58
Pure Ag	0.07	-0.52

c) 532 surfaces (kps: 4×3×1). CN: 6 at the kink.

system	$\Delta E_{NO_3}^{DFT}$	$\Delta G_{NO_3}^{EC}$
Pure Au	0.39	-0.19
1 Ag in Au(532)	0.23	-0.35
2 Ag in Au(532)	0.04	-0.55
SA 100% Ag	-0.16	-0.75
Pure Ag	-0.10	-0.68

d) 100 surfaces. We used 3×2 unit cells for the pure surfaces and the SAs (kps: 6×8×1) and 4×3 unit cells for the surfaces with adatoms (kps: 3×4×1). CN: 8 for the terraces and 5 for the adatoms (4 bonds with the surface plus one with the other adatom).

system	$\Delta E_{NO_3}^{DFT}$	$\Delta G_{NO_3}^{EC}$
Pure Au	0.68	0.10
2Au adatoms on Au(100)	0.45	-0.14
2 Ag adatoms on Au(100)	0.00	-0.59
SA 33% Ag on Au(100)	0.29	-0.30
2Ag adatoms on Ag(100)	-0.16	-0.75
Pure Ag	-0.10	-0.69

Moreover, in Figure S2 we show the different facets used in the calculations with *NO_3 adsorbed in its most stable configuration and preferred adsorption site. The facets appear in order of decreasing coordination numbers, except for the 111, shown in Figure 1 in the main text. The data in green in Table S3 corresponds in the following pictures to a case in which *NO3 binds to two Ag atoms in a Au substrate. Except for the cases of adatoms at 111 and 100 surfaces, the Ag atoms occupy substitutional positions in Au lattices.

a) 100 surface. CN: 8 at the terraces.

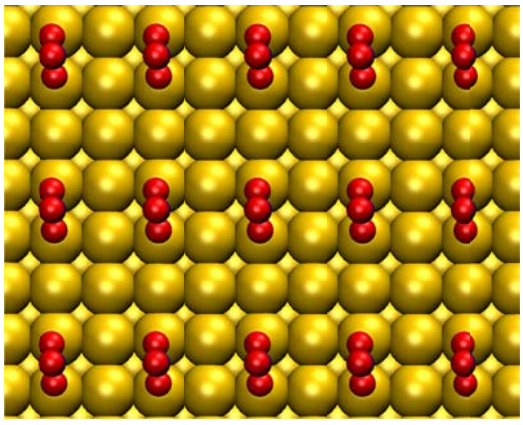

b) 211 surface. CN: 7 at the step edge.

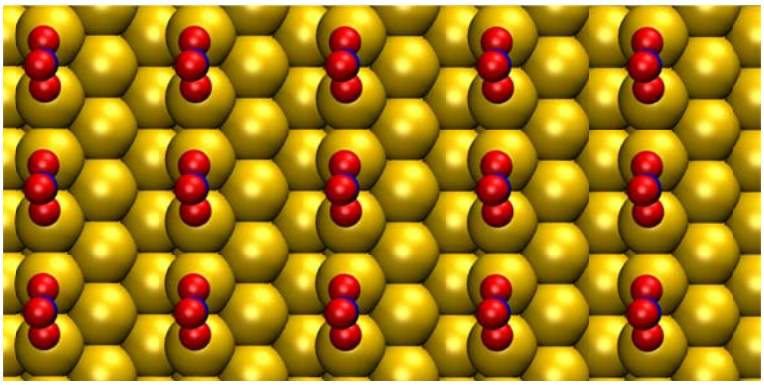

c) 532 surface. CN: 6 at the kink.

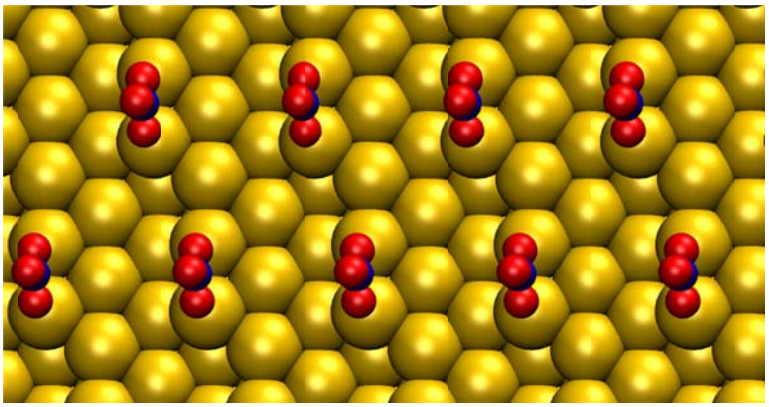

d) Adatoms in a 100 surface. CN: 5 for the adatoms (4 bonds with the surface plus one with the other adatom).

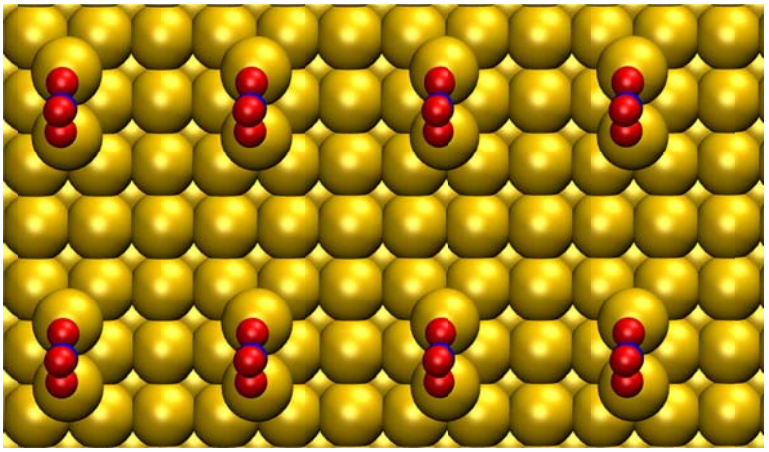

e) Adatoms in a 111 surface. CN: 4 for the adatoms (3 bonds with the surface plus one with the other adatom).

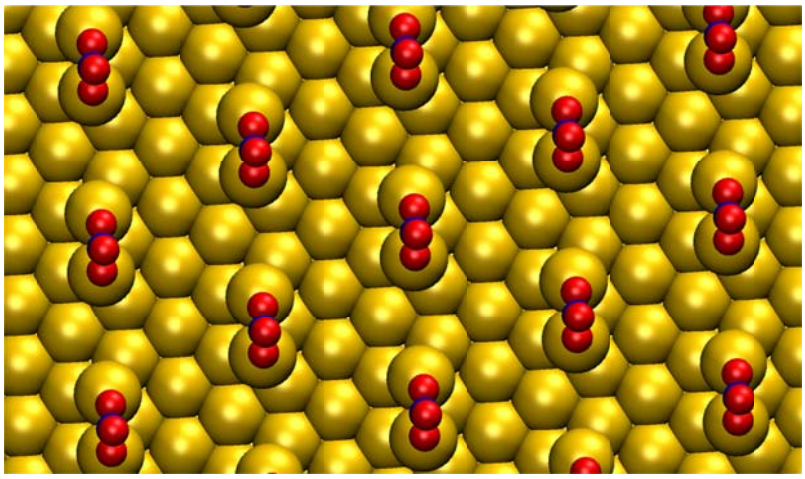

Figure S2. Schematics of the various facets used in the DFT calculations with $*NO_3$ adsorbed in a bidentate fashion in its preferred sites at the surface. The coordination numbers of the active sites are also provided.

2. Electrochemical Measurements

Before the experiments, the Au EQCM-crystal electrode was first cycled in 0.1 M $HClO_4$ between -0.67 and 1.0 V vs. MMS until characteristic cyclic voltammograms (Figure S3A), which resembles those characteristic for Au(hkl) stepped surfaces (Figure S3B) and stable QCM frequency responses were obtained. Ag atomic layer was formed on the Au electrode in a solution of 1 mM Ag^+ in 0.1 M $HClO_4$ with the UPD-technique described in [5,6]. Briefly, different Ag coverages with monolayer or submonolayer amounts on Au were obtained by scanning to different deposition potentials. After thoroughly rinsing the electrochemical cell with water, 5 mM $NaNO_3$ (99.999%, Fluka) in 0.1 M $HClO_4$ supporting electrolyte was introduced while keeping the potential control during the whole procedure. Solutions were degassed for at least 20 min with high purity Ar (Air Liquide, 5.0, Germany, supplied using Swagelok® stainless steel tubing), and all experiments were performed under a constant Ar-atmosphere.

(A)

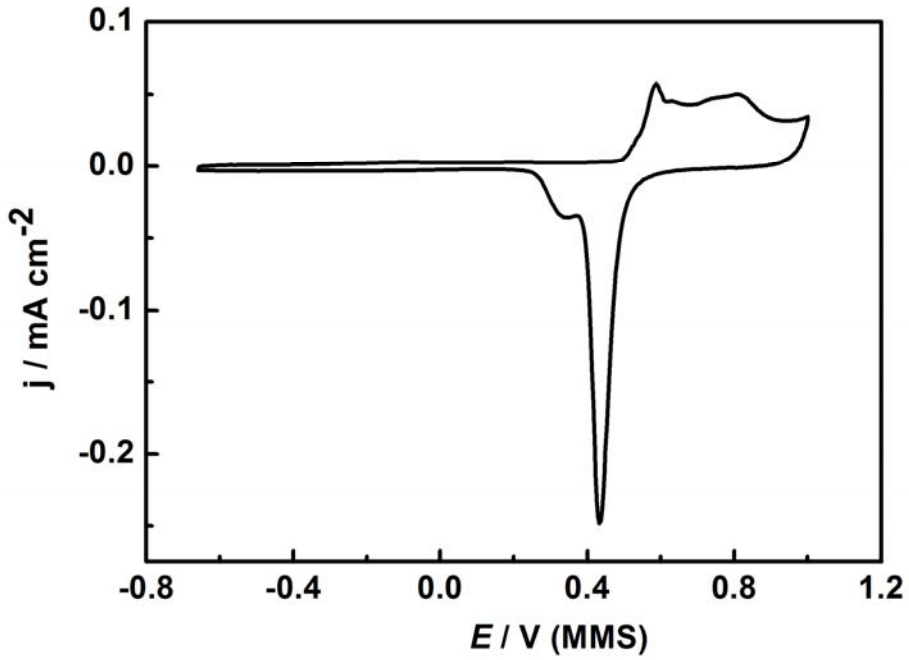

(B)

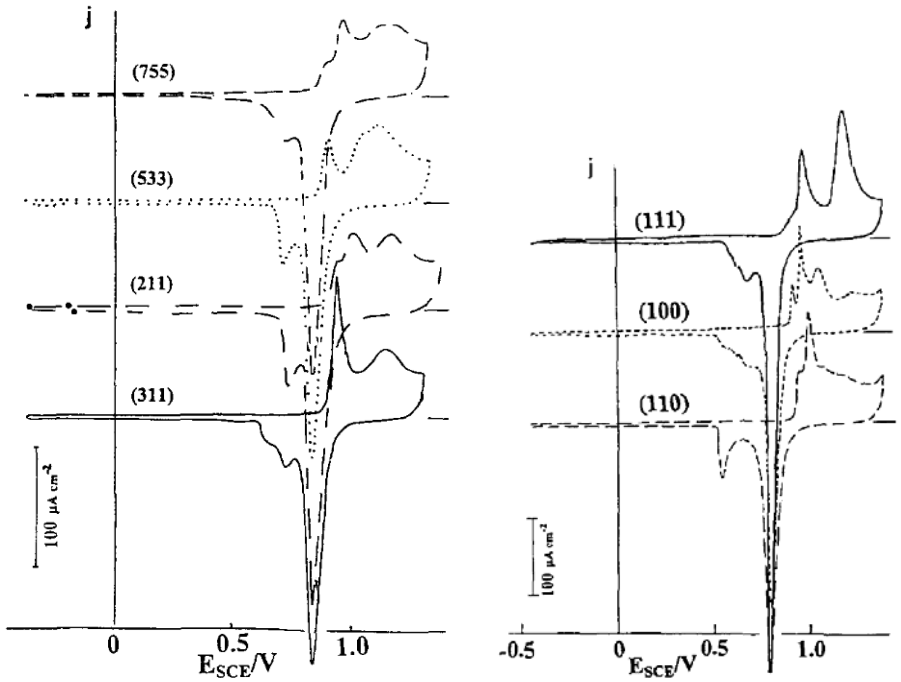

Figure S3. (A) Cyclic voltammograms of the polycrystalline Au working electrode before deposition of Ag adatoms. Electrolyte 0.1M $HClO_4$. d*E*/dt = 50 mV/s. (B) cyclic voltammograms of stepped Au(hkl) surfaces (adapted from refs [7,8])

Finally, Figure S4 illustrates the stability of measured current response caused by reduction of nitrate ions upon continuous cycling.

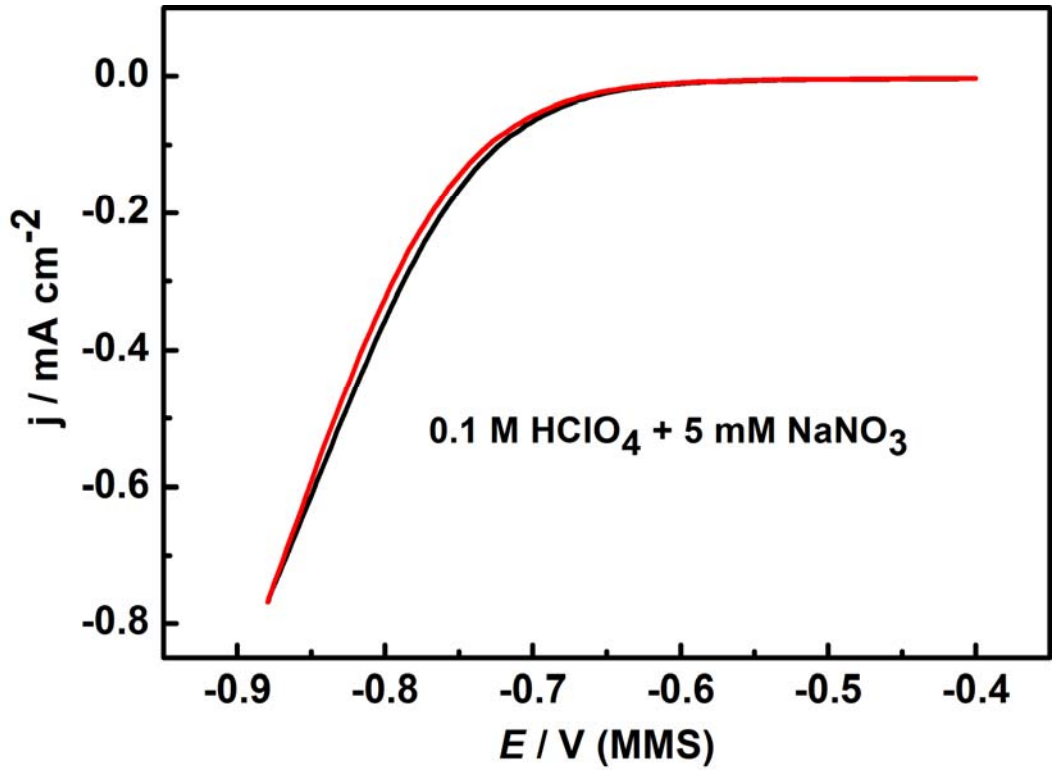

Figure S4. (A) Cathodic parts of continuous cyclic voltammograms of the Au electrode modified with ~ 0.45 ML Ag in 0.1 M $HClO_4$ + 5 mM $NaNO_3$: the first (black line) and the 25th cycles (red line). d*E*/dt = 50 mV s^{-1}.

REFERENCES

1. Norskov, J. K.; Rossmeisl, J.; Logadottir, A.; Lindqvist, L.; Kitchin, J. R.; Bligaard, T.; Jonsson, H.; *J. Phys. Chem. B* **2004**, 108, 17886-17892.

2. Lide, D. R. CRC handbook of chemistry and physics. 90th ed. 2010, Boca Raton (FL): CRC Press/Taylor and Francis.

3. Kurth, S.; Perdew, J.P.; Blaha, *Int. J. Quantum Chem* **1999**, *75*,889-909.

4. Chase, M. W.; Davies, C. A.; Downey, J. R.; Frurip, D. J.; McDonald, R. A.; Syverud, A. N.; *J. Phys. Chem. Reference data* **1985**, *14*, 1-926.

5. Berkes, B. B.; Maljusch, A.; Schuhmann, W.; Bondarenko, A. S. *J. Phys. Chem. C* **2011**, *115*, 9122-9130.

6. Huang, M.; Henry, J. B.; Berkes, B. B.; Maljusch, A.; Schuhmann, W.; Bondarenko, A. S. *Analyst* **2012**, *137*, 631-640.

7. Hamelin A., *Journal of Electroanalytical Chemistry* **1996**, *407*, 1 – 11.

8. Hamelin A., Martins, A.M. *Joumal of Electroanalytical Chemistry* **1996**, *407*, 13-21.